Significance of improved Fourier-Fick laws in nonlinear convective micropolar material stratified flow with variable properties

Muhammad Waqas [a,*], Muhammad Ijaz Khan [a], Shahid Farooq [a], Tasawar Hayat [a,b] and Ahmed Alsaedi [b]

[a] Department of Mathematics, Quaid-i-Azam University 45320 Islamabad 44000, Pakistan

[b] Nonlinear Analysis and Applied Mathematics (NAAM) Research Group, Department of Mathematics, Faculty of Science, King Abdulaziz University, P. O. Box 80257, Jeddah 21589, Saudi Arabia

*Corresponding author E-mail: mwaqas@math.qau.edu.pk (M. Waqas)

Abstract: Present research article describes the effectiveness of improved Fourier-Fick fluxes and temperature-dependent conductivity on the 2D, incompressible steady micropolar material flow over a stretchable surface. Nonlinear mixed convection, double stratification and heat generation aspects are considered. The considered flow nonlinear partial differential equations are converted to ordinary equations via appropriate transformations. Through implementation of homotopy method the obtain system is solved for series solutions. The effects of pertinent parameters are discussed through graphical sketch. Skin friction coefficient (drag force) is calculated. Main findings are pointed out.

Keywords: Improved Fourier-Fick fluxes; Micropolar material flow, Improved Fourier's expression, Double stratification; Temperature-dependent conductivity; Stagnation point flow.

1 Introduction

To elaborate the energy transportation through heat conduction, the well-known Fourier relation has been extensively applied in engineering utilizations [1]. Heat conduction expression via Fourier situation has parabolic nature which permits thermal instabilities to communicate thermal propagation of wave having infinite speed and requires to be improved at extremely smaller time scales and length in a few nano/micro-scale structures [2]. A well-known methodology in which limited velocity of thermal wave proliferation is accounted via relaxation time concept is initiated which turns heat conduction expression from parabolic form to the hyperbolic one [3-5]. Numerous researchers have contributed further developments subjected to

Cattaneo model [3]. Christov [6] modified Cattaneo model [3] via insertion of upper-convected Oldroyd's derivative. Some researches elaborating flow subjected to Cattaneo-Christov (non-Fourier) heat flux are given in Refs. [7-12].

Among numerous models of non-Newtonian materials, the micropolar material model has acquired ample consideration in view of the fact that it is capable to illustrate the micro-motions and local structure features of liquid components which are overlooked by traditional models. Several real materials (liquid crystals, animal blood, polymeric suspensions, muddy fluids, small scales water models etc.) reveal microscopical characteristics (like rotation) being effectively described through micropolar material model. From physical viewpoint, this model elaborates materials involving large quantity of tiny spherical components uniformly disseminated inside the viscous medium. Related rheological model is established on novel vector field introduction and rotating particles (microrotation) angular velocity field. Accordingly, one novel vector expression is inserted to Navier-Stokes structure coming from angular momentum conservation. Therefore, we finish off with a multifaceted (coupled) PDEs system fulfilled by velocity of fluid, microrotation and pressure with four novel viscosities established. The micropolar material model was initially modeled by Eringen [13]. Lukaszewicz [14] presents a monograph which comprehensively addresses the novel mathematical concept covering this unique model. Afterwards numerous investigators consider micropolar material subjected to distinct aspects (see Refs. [14-18]).

Here micropolar material flow near a stagnant point is formulated in frames of modified Fourier-Fick laws and heat generation. Variable fluid properties (temperature-dependent conductivity) and double stratification characteristics are considered. Homotopy solutions [19-25] are established for developed systems. Physical interpretation is given for various aspects of sundry variables against the profiles of velocity, thermal and solutal fields.

2 Formulation

Here incompressible micropolar material stagnation point flow highlighting the non-Fourier-Fick fluxes is modeled. The concept of heat generation is utilized for energy expression formulation. Double stratification and variable fluid properties (temperature-dependent conductivity) are also considered. Nonlinear version of mixed convection is introduced. Application of boundary-layer theory yields the following governing expressions [15]:

$$\frac{\partial u}{\partial x}+\frac{\partial v}{\partial y}=0, \tag{1}$$

$$u\frac{\partial u}{\partial x}+v\frac{\partial u}{\partial y}=\left(\nu+\frac{k}{\rho}\right)\frac{\partial^2 u}{\partial y^2}+\frac{k}{\rho}\frac{\partial N}{\partial y}+g\begin{pmatrix}\beta_1(T-T_\infty)+\beta_2(T-T_\infty)^2\\+\beta_3(C-C_\infty)+\beta_2(C-C_\infty)^2\end{pmatrix}+U_e(x)\frac{dU_e(x)}{dx}, \tag{2}$$

$$u\frac{\partial N}{\partial x}+v\frac{\partial N}{\partial y}=\frac{\gamma^*}{\rho j}\frac{\partial^2 N}{\partial y^2}-\frac{k}{\rho j}\left(2N+\frac{\partial u}{\partial y}\right). \tag{3}$$

$$u\frac{\partial T}{\partial x}+v\frac{\partial T}{\partial y}+\lambda_1\begin{pmatrix}u\frac{\partial u}{\partial x}\frac{\partial T}{\partial x}+v\frac{\partial v}{\partial y}\frac{\partial T}{\partial y}+v\frac{\partial u}{\partial y}\frac{\partial T}{\partial x}\\+2uv\frac{\partial^2 T}{\partial x\partial y}+u^2\frac{\partial^2 T}{\partial x^2}+v^2\frac{\partial^2 T}{\partial y^2}\\-\frac{Q}{\rho c_p}\left(u\frac{\partial T}{\partial x}+v\frac{\partial T}{\partial y}\right)\end{pmatrix}=\frac{1}{\rho c_p}\frac{\partial}{\partial y}\left(K(T)\frac{\partial T}{\partial y}\right)+\frac{Q}{\rho c_p}(T-T_\infty), \tag{4}$$

$$u\frac{\partial C}{\partial x}+v\frac{\partial C}{\partial y}+\lambda_2\begin{pmatrix}u\frac{\partial u}{\partial x}\frac{\partial C}{\partial x}+v\frac{\partial v}{\partial y}\frac{\partial C}{\partial y}+v\frac{\partial u}{\partial y}\frac{\partial C}{\partial x}\\+2uv\frac{\partial^2 C}{\partial x\partial y}+u^2\frac{\partial^2 C}{\partial x^2}+v^2\frac{\partial^2 C}{\partial y^2}\end{pmatrix}=D\frac{\partial^2 C}{\partial y^2}, \tag{5}$$

$$\begin{aligned}&u=U_w(x)=cx,\ v=0,\ N=-m_0\frac{\partial u}{\partial y},T=T_w=T_0+a_1x,\ C=C_w=C_0+b_1x \text{ at } y=0,\\&u\to U_e(x)=ex,\ N\to 0,T\to T_\infty=T_0+a_2x,\ C\to C_\infty=C_0+b_2x \text{ when } y\to\infty.\end{aligned} \tag{6}$$

Here (u,v) indicate liquid velocities (horizontal, vertical), ν kinematic viscosity, ρ liquid density, k vortex viscosity, g gravitational acceleration, N micro-rotation velocity, (β_1,β_2) thermal expansion (linear, nonlinear) coefficients, (T,T_∞) temperatures (fluid, ambient), j micro-inertia, (C,C_∞) concentrations (fluid, ambient), (β_3,β_4) solutal expansion (linear, nonlinear) coefficients, γ^* spin gradient viscosity, (λ_1,λ_2) relaxation time fluxes (thermal, solutal), (T_0,C_0) reference (temperature, concentration), (a_1,a_2,c,b_1,b_2,e) dimensional constants, Q coefficient of heat generation, m_0 boundary parameter, D mass diffusivity and c_p specific heat. The conductivity $(K(T))$ dependent on temperature is given as:

$$K(T)=K_\infty\left(1+\varepsilon\frac{T-T_\infty}{T_w-T_0}\right), \tag{7}$$

where K_∞ signify ambient fluid conductivity and ε small parameter.

Employing [11]:

$$\eta = y\sqrt{\frac{c}{\nu}},\ u = cxf'(\eta),\ v = -\sqrt{c\nu}\, f(\eta), N = cx\sqrt{\frac{c}{\nu}}g(\eta)$$
$$\theta(\eta) = \frac{T - T_\infty}{T_w - T_0},\ \phi(\eta) = \frac{C - C_\infty}{C_w - C_0}, \tag{8}$$

Eqs. (2)-(6) yield:

$$(1+K)f''' + ff'' - f'^2 + Kg' + \lambda\left[(1+\delta\theta)\theta + N(1+\delta_1\phi)\phi\right] + A^2 = 0, \tag{9}$$

$$\left(1+\frac{K}{2}\right)g'' + fg' - f'g - K(2g - f'') = 0, \tag{10}$$

$$(1+\varepsilon\theta)\theta'' + \varepsilon\theta'^2 + \Pr S\gamma_1(S_1 f' + f'\theta - f\theta') + \Pr S\theta$$
$$-\Pr(S_1 f' + f'\theta - f\theta') - \Pr\gamma_1\left(S_1 f'^2 + f'^2\theta - ff'\theta - S_1 ff'' - ff''\theta + f^2\theta''\right) = 0, \tag{11}$$

$$\phi'' - Sc(S_2 f' + f'\phi - f\phi') - Sc\gamma_2\left(S_2 f'^2 + f'^2\phi - ff'\phi - S_2 ff'' - ff''\phi + f^2\phi''\right) = 0, \tag{12}$$

$$f(0) = 0,\ f'(0) = 1,\ f'(\infty) \to A,$$
$$g(0) = -m_0 f''(0),\ g(\infty) \to 0, \tag{13}$$

$$\theta(0) = 1 - S_1,\ \theta(\infty) \to 0, \tag{14}$$

$$\phi(0) = 1 - S_2,\ \phi(\infty) \to 0. \tag{15}$$

Here $K\ \left(=\frac{k}{\mu}\right)$ denotes material parameter, $A\ \left(=\frac{e}{c}\right)$ velocities ratio, $\lambda\ \left(=\frac{Gr_x}{\mathrm{Re}_x^2}\right)$ thermal buoyancy factor, $Gr_x\ \left(=\frac{g\beta_1(T_w - T_0)x^3}{\nu^2}\right)$ thermal Grashof number, $\mathrm{Re}_x\ \left(=\frac{xU_w(x)}{\nu}\right)$ Reynolds number, $\delta\ \left(=\frac{\beta_2(T_w - T_0)}{\beta_1}\right)$ nonlinear thermal convection parameter, $N\ \left(=\frac{Gr_x^*}{Gr_x}\right)$ solutal buoyancy factor, $Gr_x^*\ \left(=\frac{g\beta_3(C_w - C_0)x^3}{\nu^2}\right)$ solutal Grashof number, $\delta_1\ \left(=\frac{\beta_4(C_w - C_0)}{\beta_3}\right)$ nonlinear solutal convection parameter, $\Pr\ \left(=\frac{\mu c_p}{K_\infty}\right)$ Prandtl number, $S_1 = \frac{a_2}{a_1}$ thermal stratified variable, $\delta = \frac{Q}{c\rho c_p}$ heat

generation variable, $(\gamma_1 = \lambda_1 c, \gamma_2 = \lambda_2 c)$ (thermal relaxation time, solutal relaxation time) factors, $S_2 = \frac{b_2}{b_1}$ solutal stratified variable and $Sc = \frac{\nu}{D}$ Schmidt number.

The coefficient of skin-friction (C_f) is expressed as

$$C_f = \frac{\tau_w}{\rho U_w^2}, \tag{16}$$

where τ_w characterizes surface shear stress provided below

$$\tau_w = \left((\mu + K) \frac{\partial u}{\partial y} + KN \right)\Big|_{y=0}. \tag{17}$$

In non-dimensional variables one has

$$\mathrm{Re}_x^{1/2} C_f = [1 + (1 - m_0)K] f''(0), \tag{18}$$

Solution procedure and convergence

Here homotopy algorithm is selected for computation of Eqs. (9)-(12) subjected to boundary conditions given in Eqs. (13)-(15). We select [15]:

$$f_0(\eta) = A\eta + (1 - A)(1 - e^{-\eta}),\ g_0(\eta) = m_0 \exp(-\eta),$$
$$\theta_0(\eta) = \exp(-\eta),\ \phi_0(\eta) = \exp(-\eta), \tag{19}$$

$$L_f = f''' - f',\ L_g = g'' - g',\ L_\theta = \theta'' - \theta, L_\phi = \phi'' - \phi, \tag{20}$$

where operators $(L_f, L_g, L_\theta, L_\phi)$ expressed in (20) have subsequent properties:

$$L_f(C_1 + C_2 e^{\eta} + C_3 e^{-\eta}) = 0,\ L_g(C_4 e^{\eta} + C_5 e^{-\eta}) = 0, L_\theta(C_6 e^{\eta} + C_7 e^{-\eta}), L_\phi(C_8 e^{\eta} + C_9 e^{-\eta}) = 0, \tag{21}$$

in which C_i $(i = 1 - 9)$ elucidate arbitrary constants.

The implemented scheme i.e. HAM involves auxiliary factors $(\hbar_f, \hbar_g, \hbar_\theta, \hbar_\phi)$. These factors effectively regulate series solutions convergence. Plots are portrayed for 13th order in Fig. 1. Suitable values for $\hbar_f, \hbar_g, \hbar_\theta$ and $\hbar_\phi$ are $-1.25 \le \hbar_f \le -0.35$, $-1.2 \le \hbar_g \le -0.65$, $-1.35 \le \hbar_\theta \le -0.45$ and $-1.3 \le \hbar_\phi \le -0.4$. Moreover, convergence of solutions is confirmed in

Table 1. Cleraly 25th order approximations are sufficient for convergence of Eqs. (9)-(12).

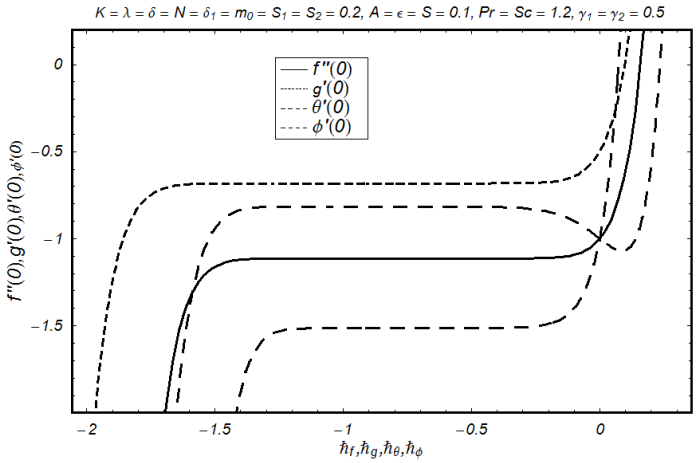

Fig. 1. $\hbar$-curves sketch for f, g, θ and ϕ.

Table 1: Convergence analysis of governing ordinary expressions for distinct order approximations when $K=\lambda=\delta=N=\delta_1=m_0=S_1=S_2=0.2, A=\varepsilon=S=0.1, \Pr=Sc=1.2$ and $\gamma_1=\gamma_2=0.5.$

order of approximations	$-f''(0)$	$-g'(0)$	$-\theta'(0)$	$-\phi'(0)$
1	1.1375	0.89375	0.9113	1.5875
5	1.1131	0.8851	0.8161	1.5176
10	1.1129	0.8853	0.8147	1.5139
20	1.1129	0.8853	0.8147	1.5139
25	1.1129	0.8853	0.8147	1.5139
30	1.1129	0.8853	0.8147	1.5139

Results

This segment elucidates the extraordinary characteristics of sundry variables versus temperature $\theta(\eta)$, concentration $\phi(\eta)$ and coefficient of skin-friction $\mathrm{Re}_x^{1/2} C_f$ via Figs. (2)-(10).

Influence of ε against $\theta(\eta)$ is scrutinized through Fig. 2. As expected $\theta(\eta)$ boosts subject to higher ε estimations. From physical perspective, liquid conductivity augments when ε is

increased. As a result, extra heat is transported towards liquid from surface and so $\theta(\eta)$ increases. Outcomes of Pr versus $\theta(\eta)$ are expressed through Fig. 3. Larger Pr estimation corresponds to less diffusivity which diminishes $\theta(\eta)$ and allied thermal layer. Fig. 4 explains γ_1 features on $\theta(\eta)$. It is witnessed that higher values of γ_1 yields $\theta(\eta)$ diminution. Here we noticed non-conducting behavior when γ_1 is augmented. Furthermore, $\theta(\eta)$ improves only for $\gamma_1 = 0$ however it reduces for $\gamma_1 > 0.$ Variations of $\theta(\eta)$ subject to S and S_1 are elaborated in Figs. 5 and 6. Clearly $\theta(\eta)$ augments for larger S whereas it diminishes subject to larger S_1. Physically, consideration of higher S provides extra heat amount in the system due to which $\theta(\eta)$ rises. Fig. 7 reports *Sc* influence on $\phi(\eta)$. One can see that $\phi(\eta)$ reduces when *Sc* is augmented. In fact the expression of *Sc* comprises mass diffusivity. In other words, an increase in *Sc* delivers lowers mass diffusivity. Hence $\phi(\eta)$ decreases. Influences of γ_2 and S_2 against $\phi(\eta)$ are disclosed through Figs. 8 and 9. These Figs. clearly demonstrate that $\phi(\eta)$ is decreasing function of larger γ_2 and S_2. Fig. 10 is portrayed to express the influences of K and m_0 versus $\mathrm{Re}_x^{1/2} C_f$. Here $\mathrm{Re}_x^{1/2} C_f$ rises when K and m_0 are increased.

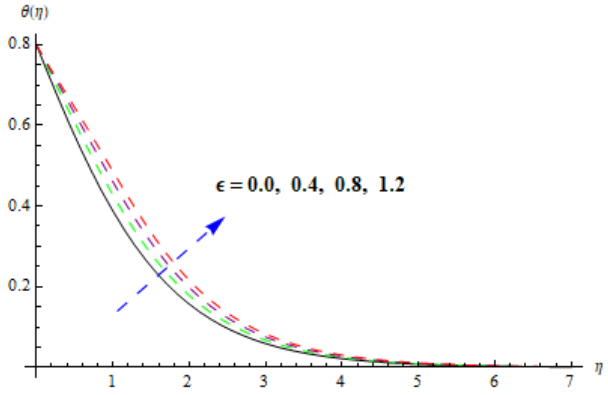

Fig. 2. ε influence versus $\theta(\eta)$.

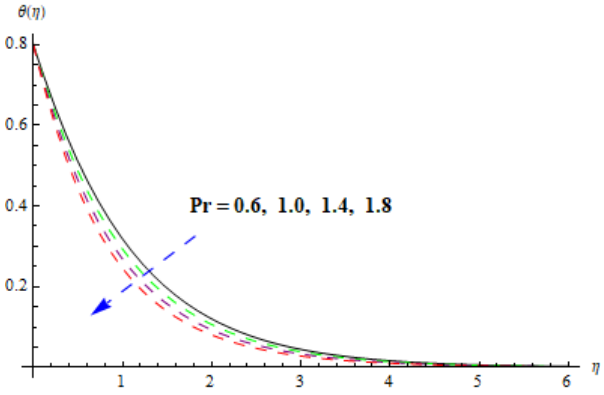

Fig. 3. Pr influence versus $\theta(\eta)$.

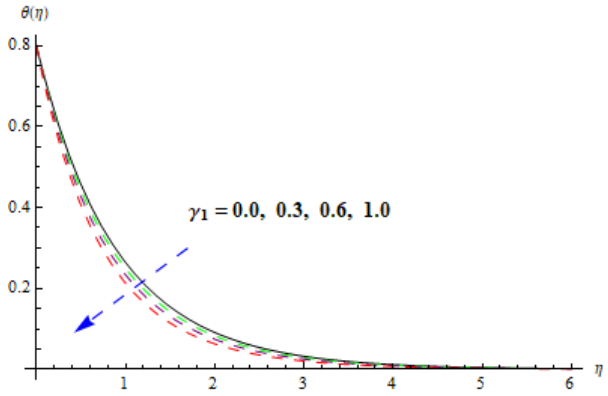

Fig. 4. γ_1 influence versus $\theta(\eta)$.

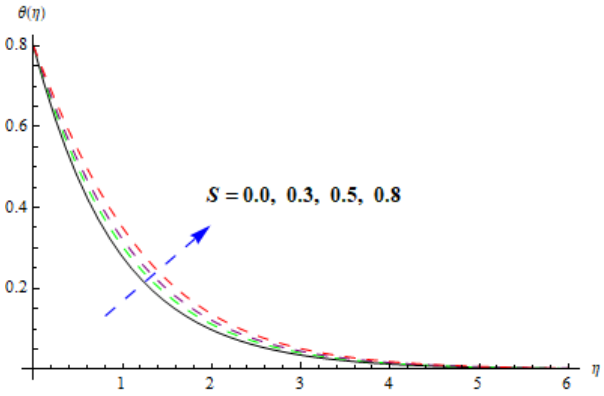

Fig. 5. S influence versus $\theta(\eta)$.

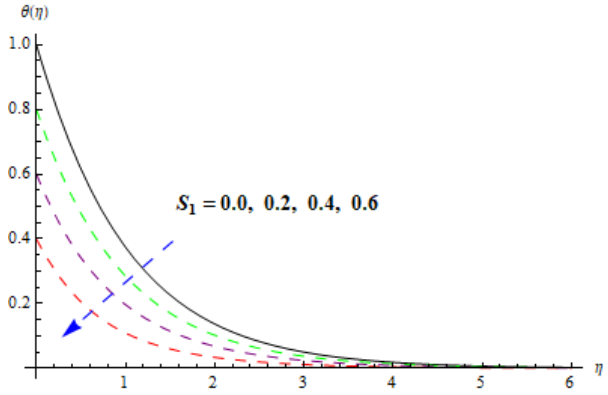

Fig. 6. S_1 influence versus $\theta(\eta)$.

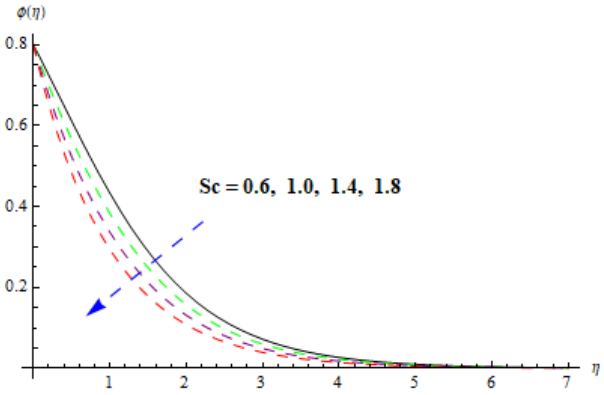

Fig. 7. Sc influence versus $\phi(\eta)$.

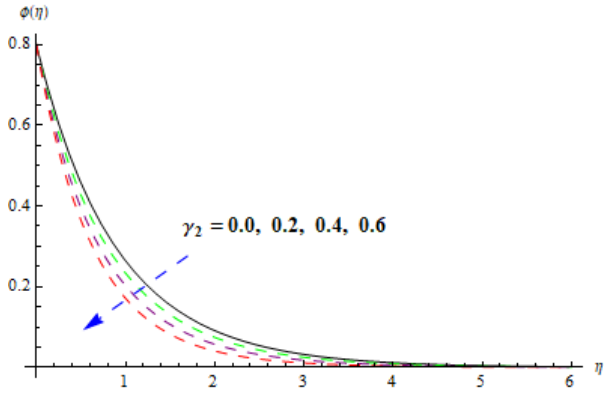

Fig. 8. γ_2 influence versus $\phi(\eta)$.

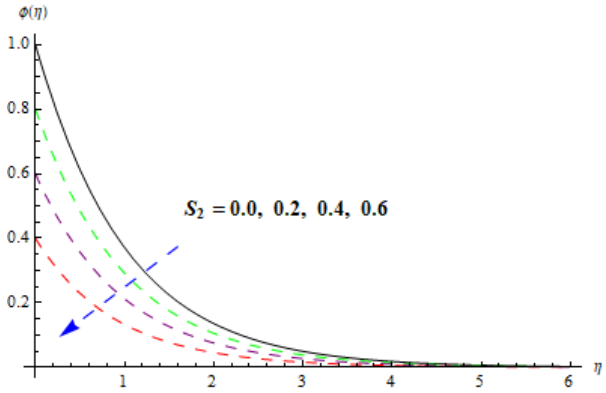

Fig. 9. S_2 influence versus $\phi(\eta)$.

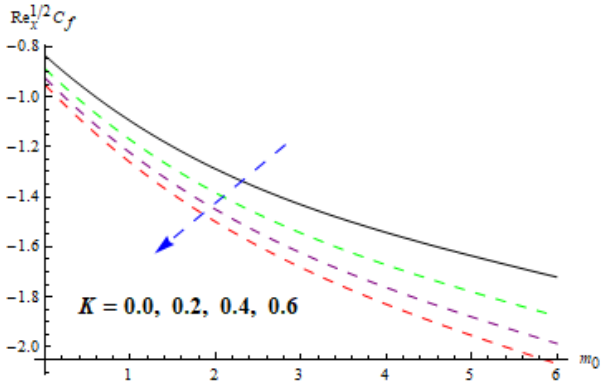

Fig. 10. K and m_0 influences versus $C_f \operatorname{Re}_x^{1/2}$.

Final remarks

The present investigation has following worth-mentioning points:

- We noticed $\theta(\eta)$ and $\phi(\eta)$ are higher in cases of $\gamma_1 = 0 = \gamma_2$ in comparison to $\gamma_1 > 0$ and $\gamma_2 > 0$.
- Consideration of higher S_1 and ε yield an improvement in $\theta(\eta)$ and $\phi(\eta)$.
- Thermal field $\theta(\eta)$ is lower for both γ_1 and $\Pr$ respectively.
- Heat generation factor (S) causes extra heat amount.
- Coefficient of skin-friction $\left(\operatorname{Re}_x^{1/2} C_f\right)$ rises when K and m_0 is enhanced.

References

1. Özisik, M. N., Heat Conduction (third ed.), John Wiley and Sons, New York (1993).
2. Chen, Z.T., Hu, K.Q., Thermo-elastic analysis of a cracked half-plane under a thermal shock impact using the hyperbolic heat conduction theory, Journal of Thermal Stresses, 35 (2012), 4, 342-362
3. Cattaneo, C., A form of heat conduction equation which eliminates the paradox of instantaneous propagation, Comptes Rendus Mathématique, 247 (1958), 431-433
4. Vernotee, P., Les paradoxes de la theorie continue de 1 equation del la Chaleur, Comptes Rendus Mathématique, 246 (1958), 3154-3155
5. Tzou, D.Y., The generalized lagging response in small-scales and high-rate heating, International Journal of Heat and Mass Transfer 38 (1995), 3231-3240
6. Christov, C. I., On frame indifferent formulation of the Maxwell-Cattaneo model of finite speed heat conduction, Mechanics Research Communications, 36 (2009), 4, 481-486
7. Straughan, B., Thermal convection with the Cattaneo-Christov model, International Journal of Heat and Mass Transfer, 53 (2010), 95-98
8. Haddad, S. A. M., Thermal instability in Brinkman porous media with Cattaneo-Christov heat flux, International Journal of Heat and Mass Transfer 68 (2014), 659-668
9. Liu, L., et al., Anomalous convection diffusion and wave coupling transport of cells on comb frame with fractional Cattaneo-Christov flux, Communications in Nonlinear Science and Numerical Simulation 38 (2016), 45-58
10. Waqas, M., et al., Cattaneo-Christov heat flux model for flow of variable thermal conductivity generalized Burgers fluid, Journal of Molecular Liquids, 220 (2016), 642-648
11. Waqas, M., et al., A generalized Fourier and Fick's perspective for stretching flow of Burgers fluid with temperature-dependent thermal conductivity, Thermal Science, (2018), doi: 10.2298/TSCI171025082W
12. Khan, M. I., et al., A comprehensive note on thermally stratified flow and non-Fourier heat flux theory, Thermal Science, (2018), doi: 10.2298/TSCI171126140K
13. Eringen, A. C., Theory of micropolar fluids, Journal of Mathematics and Mechanics 16 (1966), 1-18

14. Lukaszewicz, G., Micropolar fluids: theory and application, Birkhäuser, Boston (1999).
15. Waqas, M., et al., Magnetohydrodynamic (MHD) mixed convection flow of micropolar liquid due to nonlinear stretched sheet with convective condition, International Journal of Heat and Mass Transfer, 102 (2016), 766-772
16. Shehzad, S. A., et al., Flow and heat transfer over an unsteady stretching sheet in a micropolar fluid with convective boundary condition, Journal of Applied Fluid Mechanics, 9 (2016), 3, 1437-1445
17. Asghar, Z., et al., Rheological effects of micropolar slime on the gliding motility of bacteria with slip boundary condition, Results in Physics 9 (2018), 682-691
18. Benes, M., et al., Rigorous derivation of the asymptotic model describing a nonsteady micropolar fluid flow through a thin pipe, Computers and Mathematics with Applications (2018), doi: 10.1016/j.camwa.2018.07.047
19. Liao, S., On the homotopy analysis method for nonlinear problems, Applied Mathematics and Computations 147 (2004), 2, 499-513
20. Hayat, T., Chemically reactive flow of third grade fluid by an exponentially convected stretching sheet, Journal of Molecular Liquids 223 (2016), 853-860
21. Khan, W. A., An improved heat conduction and mass diffusion models for rotating flow of an Oldroyd-B fluid, Results in Physics 7 (2016), 3583-3589
22. Waqas, M., et al., Analysis of forced convective modified Burgers liquid flow considering Cattaneo-Christov double diffusion, Results in Physics 8 (2018), 908-913
23. Irfan, M., Modern development on the features of magnetic field and heat sink/source in Maxwell nanofluid subject to convective heat transport, Physics Letters A 382 (2018), 30, 1992-2002
24. Waqas, M., et al., Transport of magnetohydrodynamic nanomaterial in a stratified medium considering gyrotactic microorganisms, Physica B, 529 (2018), 33-40
25. Waqas, M., et al., A theoretical analysis of SWCNT-MWCNT and $_{H2O}$ nanofluids considering Darcy-Forchheimer relation, Applied Nanoscience, (2018), doi: 10.1007/s13204-018-0833-6